

Dynamic tests of Formula SAE car bodies

FILIPPO CAROLLO, GABRIELE VIRZÌ MARIOTTI, SALVATORE GOLFO, ANTONINO PAPPALARDO
Engineering Department
Palermo University
ITALY

Abstract: - Palermo University (Italy) does not participate directly in the FSAE competition, but lets its students compete "virtually" by organizing laboratories and working groups in order to design and simulate a car chassis that meets the regulations, of Formula Student in particular. These works, which flow into the students' graduate theses, are often placed together with a view to continuity and constant optimization and improvement. The purpose of this paper is to pick up the work done in the design of an automotive chassis, and to carry it out by shifting the focus no longer on the static resistance of the structure, but on the influence it has on the dynamic behavior of the vehicle. To do this, a long work of reconstruction of past models was carried out, adding to them what was necessary to complete the definition of an equivalent vehicle, and using materials and technologies used in the automotive industry. The subsequent series of simulations on three vehicles with different chassis and the comparison of the results have shown how at present the aluminum alloy frame is the preferable one over the steel and carbon alloy one.

Key-Words: Formula SAE, Structural optimization, CarSim, Simulation test,

Received: May 22, 2021. Revised: April 12, 2022. Accepted: May 10, 2022. Published: May 31, 2022.

1 Introduction

According to the Formula SAE rule [1], students have to conceive, design, manufacture and compete with a small racing car. Restrictions on the chassis and other parts of the vehicle exist to develop the knowledge, creativity, and imagination of students who have a limited budget. The cars must be built or designed within a year and have to compete with around 120 other cars from the world. The aim of the competition is to make students assume that they have been contacted by large companies to evaluate a subsequent mass production of the prototype they made (4 vehicles per day for a cost of £ 25,000). The vehicles must stand out for their good results in terms of acceleration, braking, quality of control, low production cost, easy maintenance, reliability, aesthetics.

Cars are judged during a series of static and dynamic events which include: technical inspections, costs, project presentation, technical drawing, testing and performance, high performance endurance on the track and are awarded scores for static and dynamic events. As regards the design provisions, reference should be made to the formula SAE regulation of 2021. Reference is made in particular to the characteristics of the materials and the protection against accidents.

In this paper a summary of what has been achieved at the University of Palermo (Unipa) is reported, regarding the design of a racing car according to the criteria of the SAE formula.

Over the years, the trend of optimization has led to great theoretical progress. For each of the projects examined, operations were carried out to survey the fundamental characteristics for the subsequent comparative processing.

2 The single-seater from Unipa, from 2007 to today

2.1 The steel alloy frame EVO1

The prototype Evo1, of a single-seater, was designed in 2007 [2][3][4]. This chassis prototype was created using the following materials, and the final design was determined by carrying out an optimization process in Ansys to obtain the best stiffness-weight ratio:

- Tubes material:
Steel 25CrMo4 - $E = 210 \text{ GPa}$, $\nu = 0.30$
- Main Hoop:
 $De = 25.00 \text{ mm}$; $Di = 20.00 \text{ mm}$; $s = 2.50 \text{ mm}$;
- Front Hoop:

- De = 25.00mm; Di = 20.00 mm; s = 2.50 mm;
- Absorber:
De = 15.00 mm; D1 = 12.00 mm; s = 1.50mm;
- Other tubular elements:
De = 25.00 mm; Di = 21.50 mm; s = 1.75mm;
- Wheelbase: l = 1600.00 mm;
- Maximum length: s = 2211.45 mm;
- Maximum width: b = 620,60 mm;
- Maximum height: h = 1320 mm;

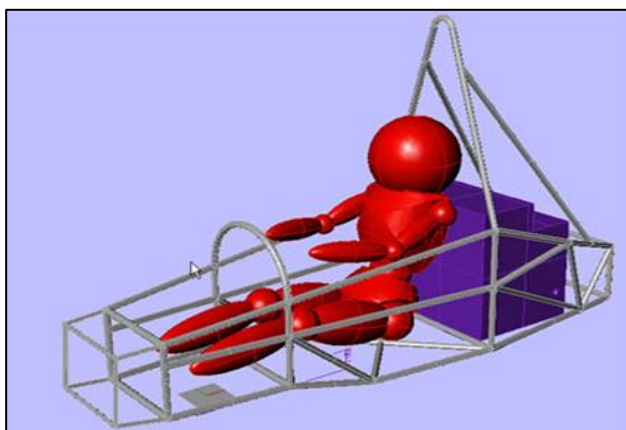


Figure 1: Perspective views of the EVO1 structure with the driver model; reinforcements and engine scheme are enclosed.

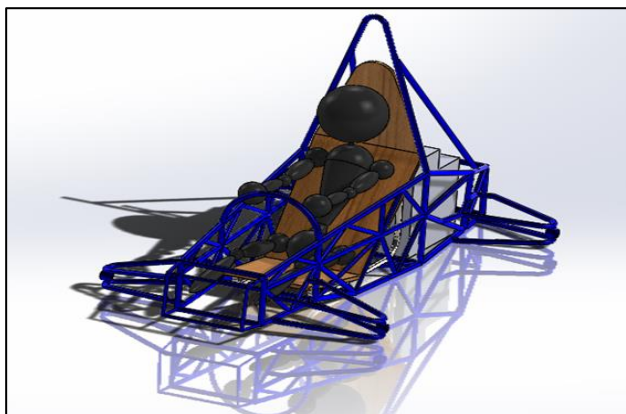


Figure 2: Perspective view of the reconstruction of EVO1

The following path is followed to reconstruct the model and execute the next elaborations:

- 1 A clear image of the photographs is acquired through the Adobe Scansi software;
- 2 The measurements of length, width and height of the drawing were taken with an electric twentieth caliper. To reduce measurement errors, each dimension was measured 10 times and the statistically most correct value was determined;
- 3 Thanks to the dimensions of point 3 and the maximum dimensions expressed in the project, the scale factor of the drawing was calculated;
- 4 At this point, each element of the 2D drawing of the frame has been measured, scaled and reproduced on Solidworks;

5 Elements outside the frame, not originally considered, have been added.

Figure 1 show the original image.

The figure 2 shows the Rendering of the rebuilt chassis, with a 95th percentile shape built according to the proportions dictated by the 2021 regulation of the FSAE, driver's seat and front and rear suspensions:

Once the model was reconstructed, the values of the suspended masses, the position of the center of gravity and therefore the main axes and moments of inertia are obtained, for the definition of the model to be used in the simulations.

- Mass = 168.43Kg;
- Position of the center of mass with respect to the point of the straight line passing through the contact points of the front wheel passing through the plane of symmetry (with Z axis length and Y axis height)
 $\Delta X = 0 \text{ mm}$ $\Delta Y = 414,18 \text{ mm}$ $\Delta Z = 1051,74 \text{ mm}$
- Principal axis of inertia and principal moments of inertia: (kg m²) In the center of the mass.
 $I_x = (0.00, 0.00, 1.00)$ $P_x = 12.75$
 $I_y = (1.00, -0.01, 0.00)$ $P_y = 49.06$
 $I_z = (0.01, 1.00, 0.00)$ $P_z = 49.72$
- Inertia Moments (kg m²) in the mass center and aligned with the resulting coordinate system
 $L_{xx} = 49.06$ $L_{xy} = -0.01$ $L_{xz} = 0.05$
 $L_{yx} = -0.01$ $L_{yy} = 49.72$ $L_{yz} = -0.12$
 $L_{zx} = 0.05$ $L_{zy} = -0.12$ $L_{zz} = 12.75$

2.2 Il telaio in tubi di alluminio EVO2

Two years later, in 2009 [5] [6] [7], the research group carried out the development of a frame, with the main objective of reducing the weight of the structure as much as possible, while maintaining high torsional stiffness parameters. To do this, 7005-T53 aluminum tubes are used for all the tubes that do not include the Main and Front Hoop, and G41 steel tubes for the two roll bars. Table 1 reports the mechanical properties of the materials used [8] [9] [10] [11] [12] [13].

Table 1: Mechanical properties of the materials in EVO2

	Alluminium 7005-T53	Steel G41
Density	$\rho = 2,78 \frac{g}{cm^3}$	$\rho = 7,87 \frac{g}{cm^3}$
Young modulus	$E = 72GPa$	$E = 210GPa$
Poisson coefficient	$\nu = 0.33$	$\nu = 0.29$
Yield stress	$\sigma_s = 370MPa$	$\sigma_s = 393MPa$
Ultimate	$\sigma_{rs} = 390MPa$	$\sigma_{rs} = 586MPa$

stress		
---------------	--	--

Tubes have the following dimensions:

- Main Hoop:
De = 25.00 mm; Di = 22.00 mm; s = 1.50 mm;
- Front Hoop:
De = 25.00 mm; Di = 22.00 mm; s = 1.50 mm;
- Aluminum tubes:
De = 35.00 mm; Di=29.00 mm; s = 3.00 mm;

The maximum dimensions of the frame are:

- Wheelbase: $l = 1600.00$ mm;
- Maximum length: $s = 2211.45$ mm;
- Maximum width: $b = 1150.00$ mm;

For this structure, the project was available in electronic format, so there was no need to scan the paper.

To obtain the data necessary for the simulations, the same procedure described in paragraph 2.1 was followed starting from point 2.

Figure 3 shows the original images and the figure 6 the reconstruction.

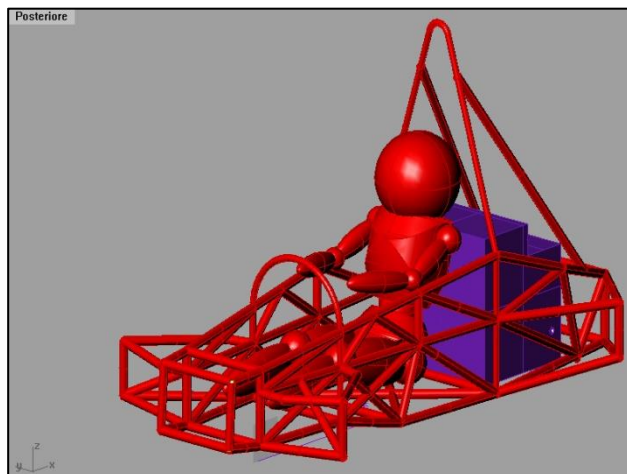


Figure 3: rendering of EVO2 frame with the pilot silhouette and engine scheme.

In reconstructing the solid model of the structure, some gaps in the original version were realized, probably born from the fact that they fell into secondary aspects for the designer's purpose

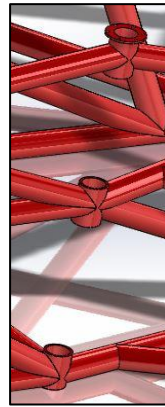


Figura 5: detail on the seat of the joint



Figura 4: detail on the thickening of the rollbar

After discarding other solutions that compromise the original characteristics as weight and flexibility, it decided to take advantage of the different diameters of the tube: the aluminum truss is initially welded whole (figures 4 and 5), with two straight tubes to simulate the straight part of the two roll bars, closed at the lower end by a welded cap, perforated in the center. A perforated flange is welded on the upper edge of the pipes, and acts as a stop. At the same time, a perforated stop flange and a perforated cap at the end are welded to the steel pipes at an appropriate height, and a second tubular is fitted at certain predetermined heights, capable of bringing the external diameter of the roll bar to coincide. with the internal diameter of the aluminum section. In this way, once the piece has been inserted by sliding into its seats, the connection is completed, preventing axial sliding by means of bolts in the upper part and a structural rivet in the lower part. It is also possible, as shown in the rendering, to remove the non-contact part of the aluminum seat, but only after the connection; this has been made to prevent the release of any residual stress from misaligning the sleeves that are formed. The corrosion problems due to galvanic currents that would arise from the contact of the two metals, the steel should first be galvanized and then painted.

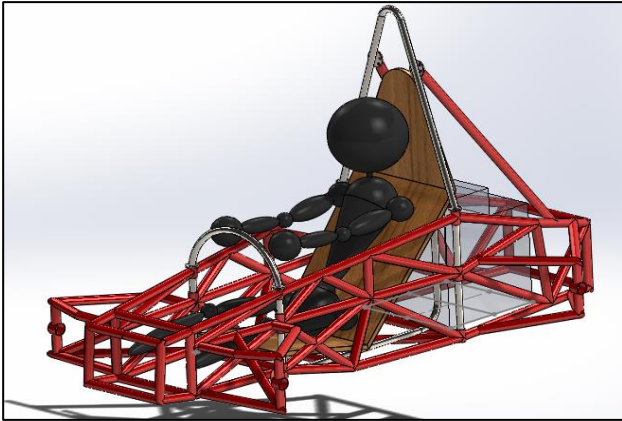


Figure 6: Perspective view of the reconstruction of the Evo2 chassis

Also for this model, the values of the suspended masses, the position of the center of gravity and axes and main moments of inertia were extracted:

- Mass = 138.29Kg;
- Position of the center of mass with respect to the mean point of the straight line passing between the contact points of the front wheel with the ground, passing through the plane of symmetry (with axis Z and Y in the direction of length and height respectively):
 $\Delta X = 0 \text{ mm}; \Delta Y = 369,4 \text{ m}; \Delta Z = 1171,43 \text{ mm}$
- Principal axis of inertia and principal moments of inertia: (kg m²) in the center of the mass.
 $I_x = (0.00, -0.04, 1.00) \quad P_x = 12.75$
 $I_y = (0.00, -1.00, -0.04) \quad P_y = 49.06$
 $I_z = (1.00, 0.00, 0.00) \quad P_z = 49.72$
- Inertia moments (kg m²) in the center of mass and aligned with the coordinate system.
 $L_{xx} = 32.37 \quad L_{xy} = 0.00 \quad L_{xz} = 0.00$
 $L_{yx} = 0.00 \quad L_{yy} = 32.04 \quad L_{yz} = -0.83$
 $L_{zx} = 0.00 \quad L_{zy} = -0.83 \quad L_{zz} = 9.41$

2.3 The frame in carbon fiber

The latest evolution of the single-seater chassis taken into consideration is designed in 2012 [14] [15], which is indicated with the initials EVO3. In this particular iteration of the problem, always keeping as target the lowering of weights with the same resistance to torsion, the idea of developing a lattice cell was abandoned in favor of a carbon fiber body.

The final developed frame has a symmetrical laminate composed of 24 sheets, 4.8mm thick and the mechanical properties in Table 2 [16] [17].

Table 2: Mechanical properties of the laminate in carbon fibre

Theoretical density	$\rho_c = 1,68 \frac{kg}{dm^3}$
Longitudinal breaking tension	$\sigma_{LR} = (V_f \cdot \sigma_f) + (V_m \cdot \sigma_m) =$

	$= 2575MPa$
Longitudinal Young's modulus	$E_L = (V_f \cdot E_f) + (V_m \cdot E_m) = 450GPa$
Transverse Young's modulus	$E_T = 27,4GPa$
Major Poisson's ratio	$\nu_L = (V_f \cdot \nu_f) + (V_m \cdot \nu_m) = 0,27$
Minor Poisson's ratio	$\nu_T = \left(\nu_L \cdot \frac{E_m}{E_f} \right) = 0.001$
Transversal breaking stress	$\sigma_{TR} = \frac{\sigma_m}{S} = 75MPa$
Transversal modulus of elasticity	$G_{LT} = 22,7GPa$

This has led to the generation of a very light frame: only 18.83kg, weighed down only by three steel reinforcements positioned halfway up the body, coinciding with the front suspension attachments and on the sides of the driver's seat, for a total of 24,83kg (figure 7).



Figure 7: the three original steel reinforcements

Also in this case, as the models no longer exist, the acquisition and measurement process had to be repeated. Less importance was given to the aspects related to the general vehicle, providing only a few dimensions on which to base the reconstruction: the distance between the backrest and the outer edge of the frame, of 450mm, the distance between the backrest and the attachment of the front suspensions to 800mm and the position of the rear axle, 400mm from the edge of the frame. The reconstruction of the model was implemented by a steel tube trellis (the same steel tubes 25CrMo4 of the first model) for the MainHoop, the front and rear suspensions, and the subframe on which they engage. The addition of these components led to the vehicle presented in figure 8. The final model has the characteristics reported in table 3.

Table 3: Characteristics of the final model in carbon fiber.

Max height	1301,41mm
Maximum length	2591,22mm
Maximum width	1230,00mm
Wheelbase	1670,00mm
Total mass	152,68kg

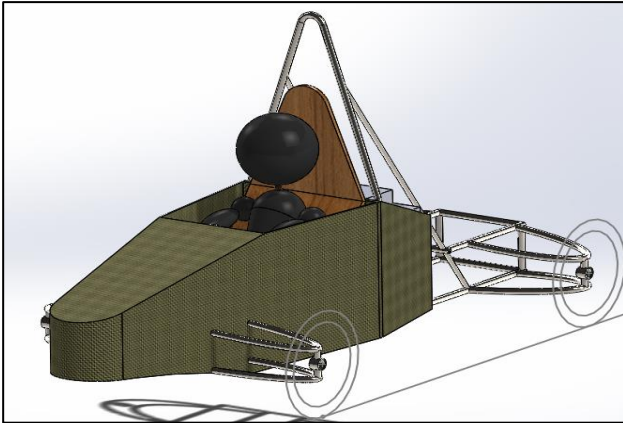


Figure 8: Perspective view of the reconstructed frame

The addition of the rear steel structure, in order to comply with the parameters of the FSAE regulation, has canceled the weight advantage compared to the aluminum frame, and also the center of mass is moved towards the rear due to the lightness of the front end, therefore the weight distribution differs from the optimum by 50% on the two axles.

This is evident in the moments of inertia encountered by the modeler:

- Position of the center of mass with respect to the mean point of the straight line passing between the contact points of the front wheel with the ground, passing through the plane of symmetry (with axis Z and Y in the direction of length and height respectively):

$$\Delta X = 0 \text{ mm}; \Delta Y = 362.46,4 \text{ mm}; \Delta Z = 868,56 \text{ mm}$$

- Principal axis of inertia and principal moments of inertia: (kg m²) in the center of the mass.

$$\begin{array}{ll} I_x = (0.00, 0.05, 1.00) & P_x = 11.80 \\ I_y = (1.00, 0.00, 0.00) & P_y = 43.16 \\ I_z = (0.00, 1.00, -0.05) & P_z = 44.29 \end{array}$$

- Inertia moments (kg m²) in the center of mass and aligned with the coordinate system.

$$\begin{array}{lll} L_{xx} = 43.16 & L_{xy} = 0.00 & L_{xz} = -0.01 \\ L_{yx} = 0.00 & L_{yy} = 44.22 & L_{yz} = 1.50 \\ L_{zx} = -0.01 & L_{zy} = 1.50 & L_{zz} = 11.87 \end{array}$$

3 Dynamic tests simulation

Knowledge of the angles characterizing the wheel alignment with respect to the ground has considerable importance since the behavior of the tire also varies with them, and therefore the dynamic behavior of the car. Since the purpose of the paper is to evaluate the influence of the chassis alone on vehicle performance, the angles are mostly standardized with the basic data provided by the software, with the exception of the angles and dimensions naturally derived from the geometry of the chassis.

CarSim [18] is a software tool developed for simulating the dynamic behavior of passenger cars and light trucks.

Uses a dynamic multi-body 3D model to accurately reproduce vehicle physics in response to driver controls. These would be steering, throttle, braking and gear shifting. Environmental conditions include a 3D earth-road surface, as well as aerodynamic and wind effects.

The mathematical models in CarSim are originally developed for mechanical engineers in the automotive industry and in research laboratories.

The intent is to reproduce the results on the test bench or on the motorway, with the same degree of reliability as that which would be obtained with repeated live tests.

CarSim uses a combination of parameters and variables to represent the vehicle. It contains special screens in which the basic parameters that can be easily measured on a real vehicle can be entered manually; the software then independently obtains the variables connected to them.

There are also tables that represent measurable properties such as suspension kinematics, tires, engine, transmission.

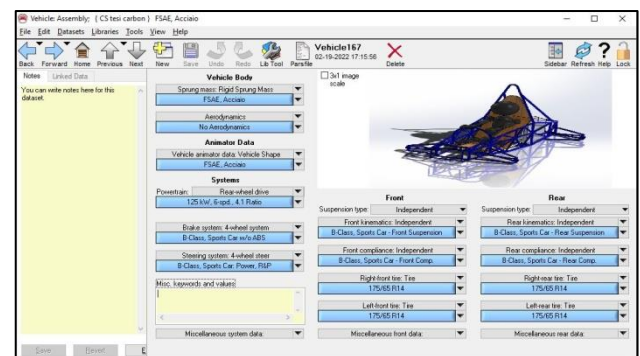
The selection of both the type of drive and the nature of the engine: internal combustion, hybrid or fully electric, is possible. CarSim comes with a database with hundreds of simulations and consists of a program file folder and a database folder.

It is possible to have multiple databases on PC.

3.1 Models, differences and similarities

Now follows the characterization, within the simulator, of the vehicles and tests. First of all, let's make explicit the steps of the simulator in which the models are characterized.

The figures 9 shows that only the menus relating to the Vehicle Body are different, in particular the Sprung masses, since it was decided to neglect the aerodynamic effects to reduce the number of variables, and Animator Data.



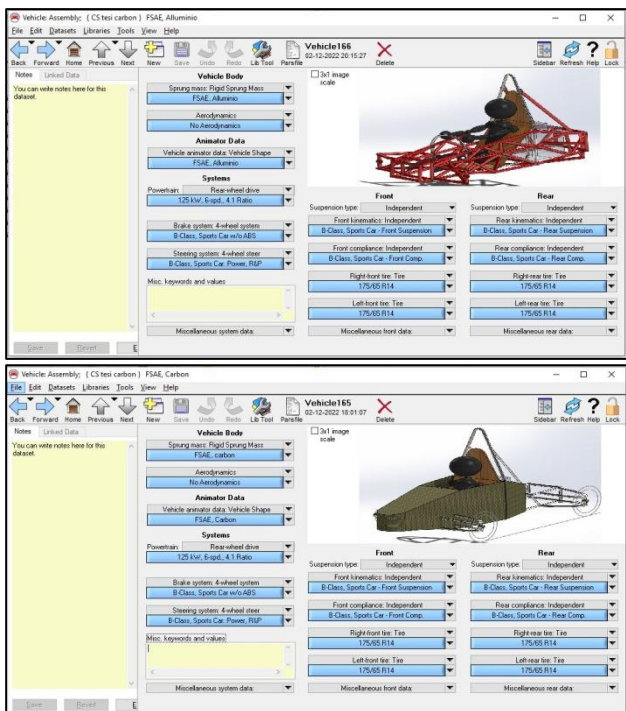


Figure 9 (a) (b) (c) :characterization of the three models: EVO1, EVO2, EVO3 from the top to the bottom

The pages relating to suspended masses are then shown in the figures 10, 11 and 12, which reflect the data presented in the previous paragraph.

The remaining specifications have been swapped from the generic B-class sports car present in the system database.

This car category includes vehicles such as the Audi TT, BMW Z4, Honda S2000, and Mazda MX-5, conceptually very close to our cars, despite higher weight, technology and power.

This choice is made in order to emphasize the dynamic effects linked to the chassis variation: having to carry out the tests under the same conditions for all three cars, it is advantageous to complete the definition of the models with the same components.

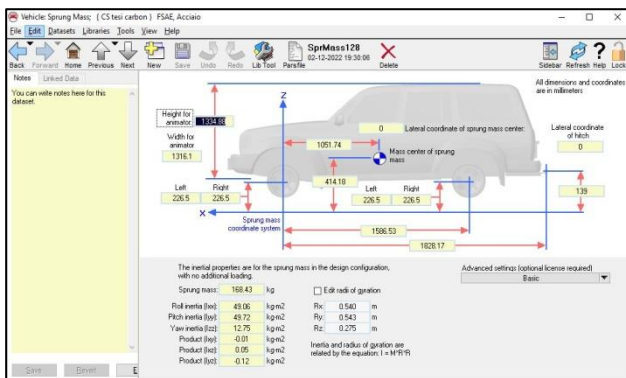


Figure 10: suspended masses and vehicle geometries of Evo1

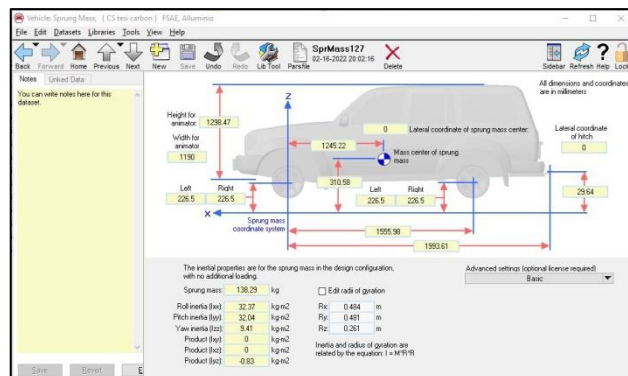


Figure 11: suspended masses and vehicle geometries of Evo2

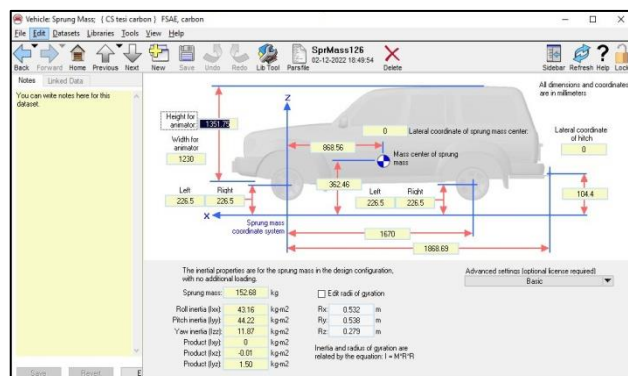


Figure 12: suspended masses and vehicle geometries of Evo3

On this assumption it seems logical to make use of pre-set and complete datasets already present in the software used, rather than designing them from the new one, an operation that is beyond the scope of this discussion.

For the sake of the brevity the screens of front and rear suspension, steering properties, braking system properties, tire characterization are missed, while the figure 13 shows the torque characteristic and the figure 14 shows the transmission ratios that are used in all the three vehicles.

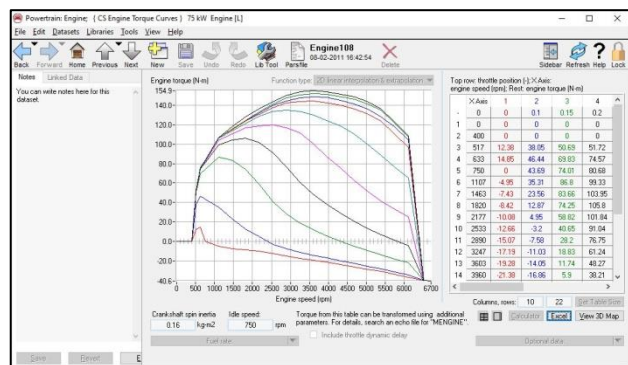


Figure 13: the engine detail page (torque characteristic).

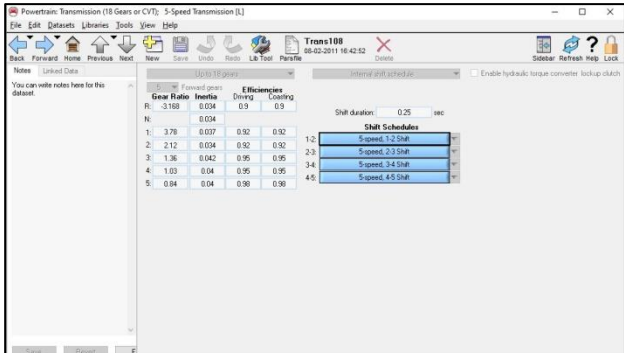


Figure 14: transmission ratios used on the three vehicles.

3.2 Selected tests

The following simulations are chosen among the many available in the software:

- **Full Throttle Acceleration:** this test was chosen in analogy with the longitudinal acceleration test provided for by the rule, and to identify the maximum speed that can be reached;
- **Understeer (ISO 4138), 40m radius:** this test was selected to evaluate the lateral acceleration of the vehicle;
- **Handling Course with Aggressive Driving:** a simulation of sports driving, which tries to evaluate the behavior of the vehicle on the track.

3.2.1 Full Throttle Acceleration

The acceleration test with the pedal fully depressed shows the behavior of the vehicle subjected to a total opening of the throttle valve.

The test conditions are:

- Test duration: 10 s
- Valve opening interval: 0.1 s
- Opening of the valve
- No intervention on the brakes
- Use of all gear ratios
- No steering intervention

The figure 15 shows the acceleration and gear ratio for the vehicle EVO1.

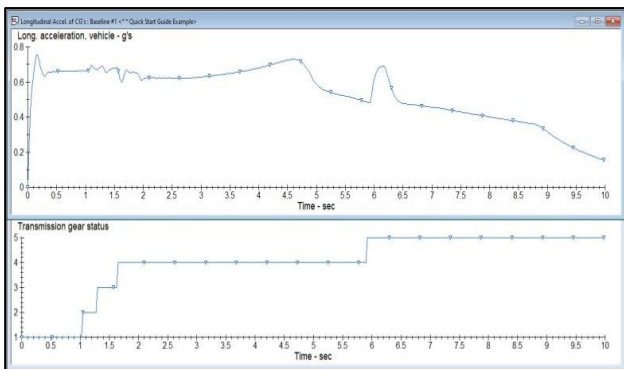


Figure 15: Acceleration and transmission ratio for EVO1

The correlation between the speed trend and the inserted transmission ratio is evident, with the acceleration decreasing as the engine runs out of delivery capacity as the engine speed increases.

Equally evident is the absence of electronic controls such as Launch Control: the speed of the rear wheels, to which the transmission is connected, shows the typical trend of skid. Top speed in this simulation is obtained equal to: $V_{Evo1} = 188.85$ km/h

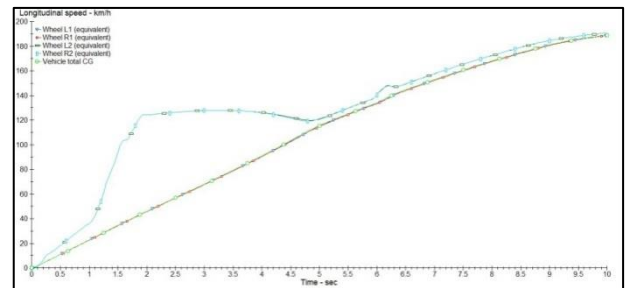


Figure 16: detail of the speed for every wheel and the vehicle Evo1

Similar trends are obtained for the second simulation, in which the tubular aluminum frame of the Evo2 is tested. They are shown in figure 17 and 18.

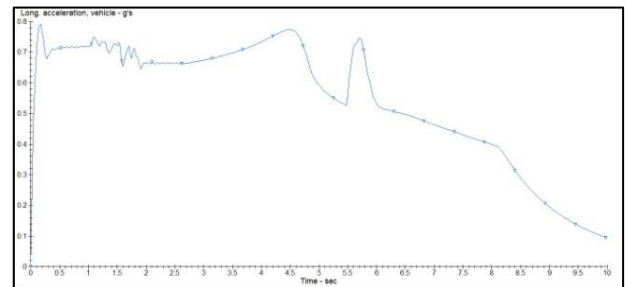


Figure 17: Acceleration versus time for Evo2

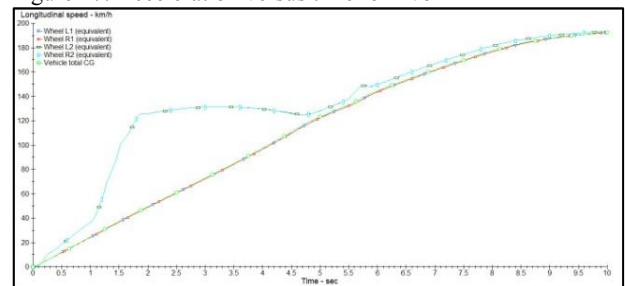


Figure 18: Speed versus time for Evo2

Maximum speed is: $V_{Evo2} = 192,43$ km/h

Figure 19 shows the difference in speed between the two previous simulations of Evo1 and Evo2.

The mass difference causes transients to be lower and top speeds higher, making the aluminum frame an optimal choice. The results obtained in the simulation of the carbon chassis are unexpected: during the test the vehicle was overturned, producing the graphs in figure 20 and 21. In the analysis phase, this result was explained as the result

of a center of gravity displaced excessively towards the rear, which meant that the lifting torques generated at maximum acceleration led to the detachment of the tires from the ground.

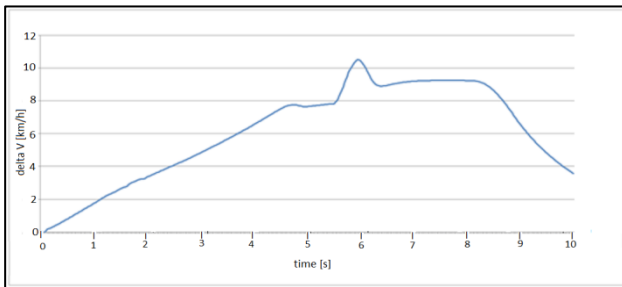


Figure 19: difference between the speeds in the two simulations of EVO1 and EVO2

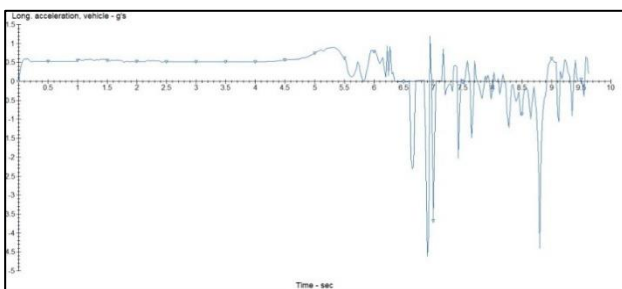


Figure 20: Acceleration versus time for Evo3

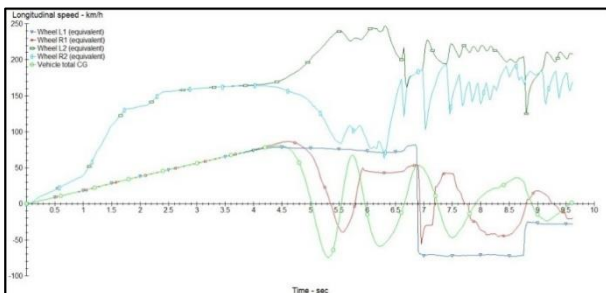


Figure 21: Speed versus time for Evo3

3.2.2 Understeer (ISO 4138), 40m radius

This test follows the directives of ISO 4138 and is used to determine the understeer behavior of a passenger vehicle.

In this case it was decided to perform the test with a constant curve radius of 40m, the value recommended as an ideal in the standard, by varying the longitudinal speed from an initial value of 10 km/h, for a test duration of 81.5 s Under these conditions it is possible to obtain the trend of the vehicle lateral acceleration, the steering angle and other parameters such as the yaw speed, the lateral slip angle and the lateral speed, the vehicle roll angle and the steering torque.

The lateral accelerations of the three vehicles are presented in the figure 22, in the order Evo1, Evo2 and Evo3.

All the three vehicles behave almost identical to each other, with the now known points of discontinuity in those instants in which the driver changes the transmission ratio, triggering a transient. A comparative overview needs the data revision in Excel.

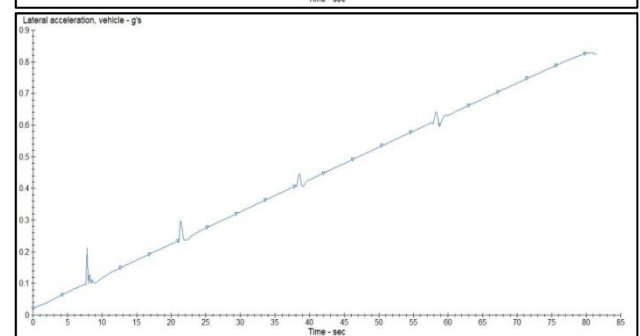
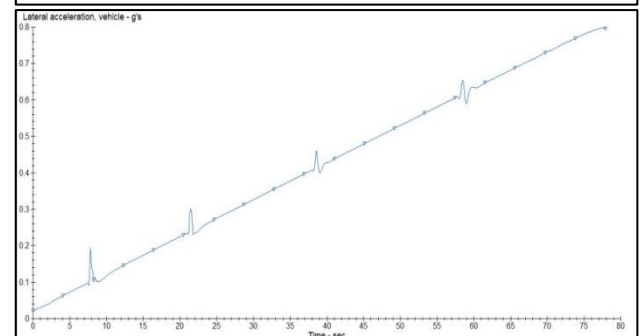
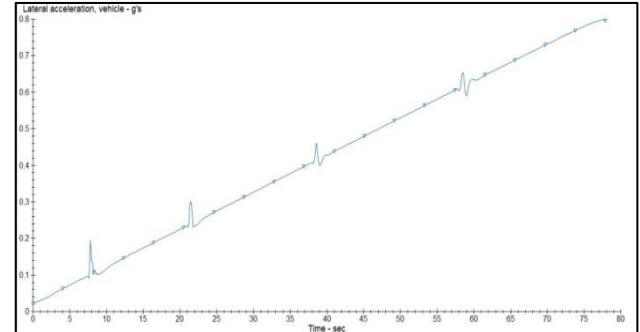


Figure 22: Lateral acceleration [g] in Understeer test; Evo1, Evo2, Evo3 from the top to the bottom.

Given that the acceleration values are given in fractions of g, and therefore the differences fall within an extremely small range of values, the use of the speeds is convenient to visualize the differences between the tests results.

The figure 23 shows the trend of the differences of the speed if the vehicles Evo2 and Evo3 by making use of the Evo1 results as reference.

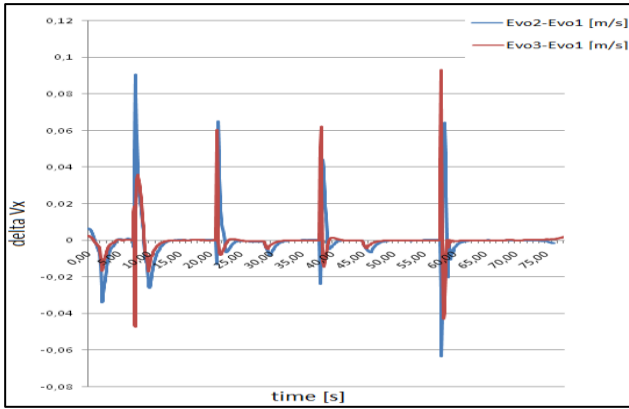


Figure 23: Speed difference of the models Evo2 and Evo3 respect to Evo1

Once again it is highlighted how the lower inertia leads the Evo2 and Evo3 to be on average faster than the Evo1, a value that is exacerbated in transients, even if the order of magnitude of these improvements is really small.

3.2.3 Handling Course with Aggressive Driving

Track test involves a lap on the track that uses the control function of CarSim named "Target speed from route preview".

It calculates a speed target over a specified preview distance, to maintain lateral and longitudinal acceleration within the specified limits.

Control of the throttle, brakes and steering is still achieved through the closed loop controls of speed and of the steering trajectory.

The target speed is closely linked to the exact geometry of the path, so the maintenance of the trajectory must also be closely linked to it and the "look ahead" distances are short. In the case under analysis, the path is a set of X-Y coordinates (which could be obtained from GPS or other tools), but a path can also be specified as an offset from a road reference.

The test path is shown in figure 24.

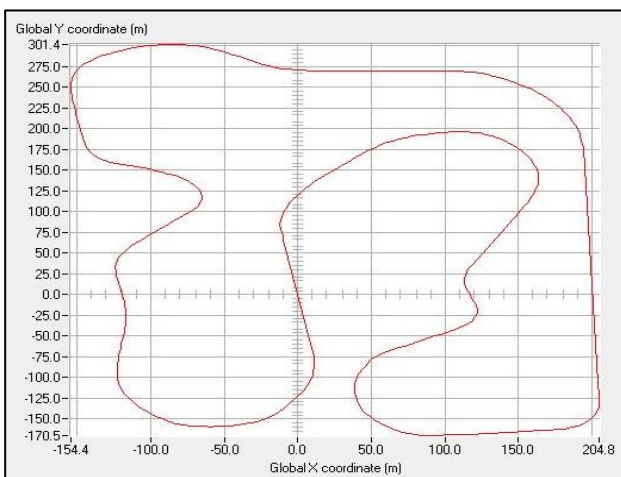


Figure 24: Simulation test circuit

A check is carried out at each step to make sure that the vehicle is following the route correctly.

If the lateral deviation reaches a certain threshold, set with the "Lat_Tolerance" parameter, the run stops.

The simulation is set to record exactly one lap.

It is necessary to set the driving logic, the intervals chosen to provide for speed control and the maximum lateral and longitudinal acceleration values allowed in the test.

The following results are collected:

- The space traveled in the time interval of 141.25 s; figure 25 shows the space difference of Evo2 and Evo3 respect to Evo1, while the maximum values are:
 1. Evo1 – 2273,45 m
 2. Evo3 – 2273,04 m
 3. Evo2 – 2272,57 m

The fact that the Evo2 vehicle is in third position should not be surprising, because, as explained in the introductory paragraph to the test, the control of trajectory, speed and acceleration follows a logic of foresight on the track, and the acceleration and deceleration logics is practically identical in the three tests and do not exploit the qualities of the three vehicles.

Therefore, for the same duration of the transient, the vehicle with lower inertia (the Evo3) undergoes a greater variation; (the speeds are compared in the figure 26).

Given that the cars are equipped with virtually the same identical components except for the chassis, it is evident that the deceleration transients affect more than the acceleration ones, resulting in a slightly lower average speed.

- Trend of the longitudinal speed V_x with respect to the trajectory and in the lap time, from which the V_{max} of the three vehicles:
 1. Evo3 - $V_{max}=116,75$ km/h
 2. Evo2 - $V_{max}=116,71$ km/h
 3. Evo1 - $V_{max}=116,71$ km/h

while the deviations at each instant of Evo2 and Evo3 respect to Evo1 are also shown in figure 25.

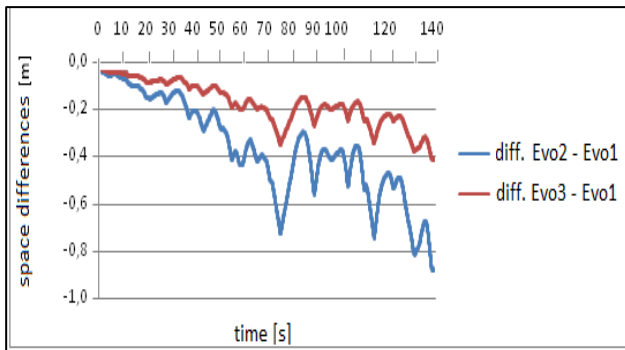


Figure 25: Differences between the space traveled over time between the simulations Evo1, Evo2, Evo3

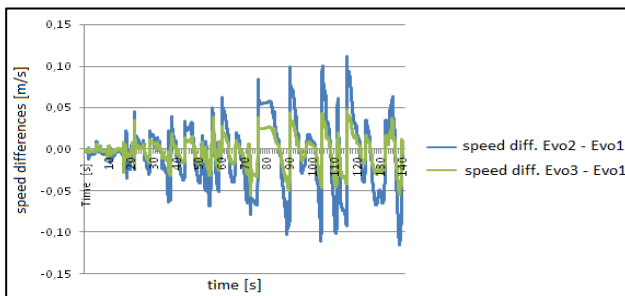


Figure 26: Difference between speeds in lap time

4 Conclusions

The work in this paper is the beginning of a process of recovering all those technical knowledge and skills related to the automotive world, that in recent years have been developed in the local context of the University of Palermo, with the aim of demonstrating that the team is ready to move on to the actual construction phase.

The work of data recovery and reconstruction of models born in past years as a case study for their own sake, disconnected from the problems of economic feasibility, technical implementation and, even worse, from the concert of parts that make up the "universe-machine" of which act as a skeleton, has allowed the creation of a database useful for the development of automotive components, with a view to modularity and integration.

For example, it is now possible to design a steering system with the awareness that it is installed on a virtually existing vehicle, with predetermined geometries and dimensions that cannot be ignored. From this same perspective, advantages can be obtained, in terms of context, in the realization of a suspension scheme, in the evaluation of the dimensions of an engine, in the estimation of the forces that this can safely discharge on its anchor points.

CarSim software allows to check whether or not the individual components can work in synergy,

obtaining maximum efficiency in a test field that simulates reality. Considering the little consolidated experience with the team program and the almost total absence of useful material in the public domain on the net, the result of this work have given great satisfaction.

Despite the many potentialities of the program still unexplored and the simplifications adopted for the purpose of the paper, it was still possible to bring to light problems that, in the original projects for their own sake, would have remained dormant.

For example, the acceleration test of the Evo3 highlighted a major flaw in the chassis: the carbon fiber frame, despite the very high level of optimization, turned out to be the worst choice once coupled to a superstructure that is not efficient enough (the overturning occurred in the acceleration test).

The database of information collected and processed in this work, as well as the experience gained in the field of simulation, allows future team participants to aim for the development of an efficient model in all its aspects. Finally, with a view to a substantial investment of resources in the Automotive field, the acquisition of the module specially developed for the Formula SAE competition by CarSim, of which Mechanical Simulation, the software house, is the official sponsor, could be evaluated.

This tool, in the hands of a consolidated team accustomed to working in a perspective of interchange and integration, allows not only to readjust and verify pre-existing models, but also to create a real prototype thanks to the reduction of the time required for theoretical development. of the components of the vehicle.

References:

- [1] Formula SAE® Rules 2020, www.fsaeonline.com
- [2] Montaperto S., *Modellazione Solida e progettazione strutturale di un telaio per autovettura di Formula SAE*, graduate thesis, Palermo University, Italy, a.y. 2006/2007
- [3] Ingrassia T., Marannano G., VirziMariotti G. - Design and Optimization of a Chassis for a Formula SAE Race Car - Proceedings 12th EAEC Congress, Bratislava, June 29- July 1, 2009
- [4] Ingrassia T., Marannano G., Montaperto S., Virzi Mariotti G. - Progettazione ed ottimizzazione di un telaio per vettura di Formula SAE - XXXVII Convegno Nazionale AIAS, Rome, 10-13 september 2008.

- [5] Caramanno R., *Costruzione di telai per autoveicoli con materiali alternative*, graduate thesis, Palermo University, Italy, a.y. 2007/2008
- [6] Lo Vetere S.A., *Progettazione e sviluppo del telaio di un autoveicolo di Formula SAE*, graduate thesis, Palermo University, Italy,, a.y. 2008/2009
- [7] Casi L., *Progetto e costruzione di telaio di vettura F.SAE: parte posteriore*, graduate thesis, Alma Mater Studiorum – Bologna University, Italy, a.y. 2009/2010
- [8] Ducker Frontier: Auto aluminum content to grow 12% by 2026, expect more closures, fenders, repairerdrivennews.com, <https://www.repairerdrivennews.com/2020/10/16/duckerfrontier-auto-aluminum-content-to-grow-12-by-2026-expect-more-closures-fenders/>, (consulted 7/24/2021)
- [9] Magnesium Alloys In Automotive Market: Market Size, Trends and Growth Analysis, lucintel.com, <https://www.lucintel.com/magnesium-alloys-in-automotive-2020.aspx>, (consulted 9/28/2021)
- [10] Barcellona A., *Tecnologie generali dei materiali*, EVerus, Palermo, 2007
- [11] Traverso M., *Progettazione di telai automobilistici Space Frame in lega leggera con particolare riguardo a soluzioni di tipo modulare*, graduate thesis, Roma "La Sapienza University, Italy, a.y. 2000/2001 <http://www.marcotraverso.it/spaceframe>
- [12] Tisza M., Czinege I., *Comparative study of the application of steels and aluminum in lightweight production of automotive parts*, in International Journal of Lightweight Materials and Manufacture, Vol. 1, Issue 4, December 2018, Pages 229-238
- [13] Light weighting, a new trend in the automotive driving aluminum demand round the globe, STAS.com, <https://www.stas.com/en/news/blog/lightweighting-a-new-trend-in-the-automotive-driving-aluminium-demand-around-the-globe/>(consulted 7/24/2021)
- [14] Costantino S.A., *Progetto di telaio in fibra di carbonio per autoveicolo di Formula SAE*, graduate thesis, Palermo University, Italy, a.y. 2011/2012
- [15] Munaretto P., *Studio di materiali compositi per l'industria automobilistica*, graduate thesis, Padova University, Italy,, a.y. 2010/2011
- [16] <https://www.slideshare.net/PadmanabhanKrishnan2/automotive-materials-kp>, (consulted 7/13/2021)
- [17] <https://www.yuk4woo.com/2020/08/06/qual-e-stata-la-prima-automobile-ad-impiegare-un-telaio-in-fibra-di-carbonio/>, (consulted 7/24/2021)
- [18] Introduction to CarSim: Part 1-Overview, YouTube, <https://www.youtube.com/watch?v=x9EeGjy9uZc>, (consulted 12/05/2021)

Creative Commons Attribution License 4.0 (Attribution 4.0 International, CC BY 4.0)

This article is published under the terms of the Creative Commons Attribution License 4.0
https://creativecommons.org/licenses/by/4.0/deed.en_US